An Acad Bras Cienc (2021) 93(4): e20201140 DOI 10.1590/0001-3765202120201140
Anais da Academia Brasileira de Ciências | *Annals of the Brazilian Academy of Sciences*
Printed ISSN 0001-3765 I Online ISSN 1678-2690
www.scielo.br/aabc | www.fb.com/aabcjournal

ENGINEERING SCIENCES

Investigation of attributes of bourbon oil and cobalt nitrate constituted electrospun nanoscaffolds for blood compatibility and in vitro bone formation

SARAVANA K. JAGANATHAN & MOHAN P. MANI

Abstract: This work aims to fabricate scaffold using polyurethane (PU) integrated with bourbon oil (BB) and cobalt nitrate ($CoNO_3$) using the electrospinning technique. Morphological investigation signified a fall in fibre diameter for the PU/BB and PU/BB/$CoNO_3$ nanocomposite than the PU. Spectral analysis indicated that BB and $CoNO_3$ were added within the PU matrix. Wettability analysis insinuated an increase in the hydrophobic nature of the PU/BB than the PU. PU/BB/$CoNO_3$ turned to be hydrophilic due to the integration of $CoNO_3$ in the polymer matrix. Mechanical testing of PU/BB and PU/BB/$CoNO_3$ indicated an increase in the tensile strength of the fabricated composites. Atomic force microscopy (AFM) portrayed the reduction in the roughness of the PU/BB and PU/BB/$CoNO_3$ compared to the PU. The coagulation studies invariably documented the improved anticoagulant behaviour and less toxic nature of the PU/BB and PU/BB/$CoNO_3$ in comparison with the PU. Further, bone mineralization testing revealed the enhanced apatite formation of the nanocomposite. Nanocomposite scaffolds with the fore-mentioned properties hold good potential for bone tissue engineering.

Key words: PU, $CoNO_3$, bourbon oil, Electrospun Scaffold, bone tissue applications.

INTRODUCTION

Owing to the limited self-regenerative potential, mostly large-sized bone defects cannot heal on their own (Neffe et al. 2014). Major defects due to trauma or infection (osteomyelitis) are treated using autografts, allografts and xenografts which are the golden standard procedures. Their several drawbacks such as disease transfer, inadequate availability and reproducibility, donor availability and immune rejection hindered their widespread application in clinics (Bokov et al. 2018). Researchers were constantly experimenting with several alternative methods for the past few decades in order to overcome the limitations of those conventional methods. Recently, tissue engineering has served as a valuable option that uses majorly three components for a reconstruction of the damaged tissues. The three lead components that are vital for any tissue engineering applications are scaffolds, cells and growth factors. Among these components, scaffold plays a major role in the cellular attachment and proliferation for de novo tissue growth (Amini et al. 2012, Ho-Shui-Ling et al. 2018).

A number of manufacturing techniques are used for the fabricating scaffolds and some to name are salt-leaching, phase separation, and sintering, etc. (Haider et al. 2020, Kundu et al. 2014). Anatomy of the bone tissue reveals that it is a complex material comprising collagen fibres, nano-hydroxyapatite and bone cells with structures ranging from nano-scale to macroscale

(Gong et al. 2015). However, scaffolds made from the above-mentioned methods fail to resemble the native structure of the bone. One of the techniques which have been known for more than a century but recently gained attention in tissue engineering application is electrospinning (Hong et al. 2019). Electrospinning apparatus comprises components like a syringe with a needle, syringe pump, high voltage supply unit and a collector (Perrone 2012). Electrospinning is a method to produce the nanofibres from various polymeric materials that can mimic the native structure of bone tissue, thanks to their outstanding properties like increased surface/volume ratio and highly connected pore density. Electrospun scaffolds are found to enhance the cell adhesion paving way to increased bone tissue growth (Jun et al. 2018, Liu et al. 2013, Vasita & Katti 2006). Polyurethane is used in this study as a base material for manufacturing scaffold as it has long-standing applications in medicine. Moreover, the polymer chosen in this study is a polyether-based medical-grade polyether which has displayed some good physicochemical properties and widely experimented for tissue engineering applications (Jaganathan et al. 2017, 2018, 2019).

Bourbon oil was obtained from the geranium bourbon through steam distillation of the leaves and stalks. The oil is sweet with pale olive-green colour (Available at: https,//www.essentialoilscompany.com/products/geranium-oil). The components present in the oil were geraniol, citronellol, isomenthone, 10-epi-γ-eudesmol and geranyl formate (Verma et al. 2013). The oil is used in skincare for normalisation of sebum levels in dry or greasy skin and it is found to stimulate the cell renewal. It acts as an adaptogen which strengths the immune, nervous and glandular system of the human body thereby resulting in enhancing the resistance to stress (Available at: https,//www.essentialoilscompany.com/products/geranium-oil). The utilization of bourbon type geranium essential oil in regenerative medicine was not reported although it provides a wide spectrum of medicinal applications. In recent years, cobalt has attracted huge attention owing to its novel electric and catalytic properties. Cobalt is widely applied in advanced batteries, supercapacitors, solar cells, electrochromic and tribological property improvement (Madani & Hamouda 2016). Also, cobalt has been reported to possess antiviral and antibacterial properties (Chang et al. 2010). Another interesting property to note is that cobalt has the ability to stimulate the angiogenic factors by influencing the hypoxia-like response (Wu et al. 2012). This research work for the first time will manufacture a scaffold based on polyurethane mixed with bourbon oil and cobalt nitrate. This work will attempt manufacturing PU/BB and P/BB/$CoNO_3$ nano-scaffolds which will be further studied for its physicochemical and in-vitro bone -forming properties.

MATERIALS AND METHODS

Materials

Tecoflex EG-80A (PU) was supplied from Lubrizol and the solvent dimethylformamide (DMF) was purchased from Sigma Aldrich, UK. Bourbon oil (Paradigm Mall, Johor), Cobalt nitrate, (Sigma-Aldrich, Malaysia), Clotting reagents (Thermo Fisher Scientific, Selangor, Malaysia) were used in this work.

Solution preparation and fabrication of nanocomposites

Electrospun PU was manufactured at 9 wt% using DMF and stirred for 12 h. For bourbon oil, 4% v/v and 4% w/v of cobalt nitrate was utilized to make solutions. PU/BB and PU/BB/$CoNO_3$ solutions were prepared by mixing bourbon oil

and cobalt nitrate solution into PU solution at a ratio of 8:1 v/v% and 8:0.5:0.5 v/v respectively and stirred. All solutions were spun at constant parameters: 0.2 mL/h (flow rate), 10.5 kV (applied voltage) and 20 cm (collector distance).

CHARACTERIZATIONS

Morphology investigation

Field Emission Scanning electron microscopy (FESEM, Hitachi SU8020) was used to picture the morphologies of fibres fabricated through electrospinning. Briefly, samples of PU, PU/BB, PU/BB/$CoNO_3$ were cut and coated with gold to improve the quality of images obtained.

Fourier transform infrared analysis (FTIR)

Nicolet FTIR spectrometer recorded IR spectra of the PU, PU/BB, PU/BB/$CoNO_3$. The electrospun composite and the PU were scanned at a wavelength between 600 and 4,000 cm^{-1}.

Contact angle measurements

Video contact angle (VCA) optima contact angle equipment was used to record the wettability of the PU, PU/BB, PU/BB/$CoNO_3$. Briefly, a water droplet (of size 5 µL) was placed on the small cut piece of the samples and its image is recorded. The contact angle was calculated through software installed in the machine.

Thermogravimetric analysis (TGA)

The thermal property investigation of the PU, PU/BB, PU/BB/$CoNO_3$ was carried out in the TGA equipment. The heating was performed by placing 3 mg of samples in the TGA unit from 30°C to 1000°C under N_2 atmospheric conditions.

Atomic force microscopy analysis (AFM)

AFM setup measured the surface roughness of the electrospun nanofibres. A small section ofthe PU, PU/BB, PU/BB/$CoNO_3$ was scanned in the tapping mode under normal atmosphere. JPKSPM data processing software was used to measure the surface roughness.

Mechanical testing

Electrospun PU, PU/BB, PU/BB/$CoNO_3$ was tested for their mechanical properties using the Gotech Testing Machine, AI-3000. Testing was performed by following the ASTM D882 standard. Samples were fixed at the gripping units of the tester and it was tested at a crosshead speed of 10mm/min with the load cell of 500 N.

Blood compatibility measurements

To determine the activated partial thromboplastin time (APTT) of the fabricated bone scaffolds (PU, PU/BB, and PU/BB/CoNO3), 50 µl of platelet - poor plasma (PPP) was placed on the surface at 37°C. This is followed by the addition of 50 µl of rabbit brain cephalin and kept incubated for 3 minutes before the addition of calcium chloride (0.025M). For prothrombin time (PT) assay, PPP addition is followed by the addition of 0.9% sodium chloride (NaCl)–thromboplastin containing calcium. In the case of haemolysis assay, a 4:5 v/v% ratio of citrated blood and diluted saline was used for incubating the samples at 37°C for 1hour. Haemoglobin released from red blood cells is estimated by measuring the optical density at a wavelength of 542nm (Mani et al. 2018, Chao et al. 2018).

BIOACTIVITY TEST

Bone forming ability was investigated by the formation of apatite. Briefly, nanofibres of PU, PU/BB, PU/BB/$CoNO_3$ with the size of 1 X, 1 cm^2 was cut and left in 1.5x SBF (pH 7.4; 37 °C) for fourteen days. Simulated body fluid (SBF) was prepared by dissolving the reagents in the distilled water to mimic the human plasma

concentrations. Briefly, 141 mM NaCl, 4.0 mM KCl, 0.5 mM MgSO4, 1.0 mM MgCl2, 4.2 mM NaHCO3, 2.5 mM CaCl2·2H2O, 3.94 g/L of Tris-HCl and 1.0 mM KH2PO4 used to prepare the SBF and pH of the solution was adjusted to 7.4 (Park et al. 2017). Fibres were removed and dried before imaging using FESEM to estimate the amount of calcium deposition.

RESULTS AND DISCUSSION

FESEM results

FESEM images (Figure 1) revealed nanofibres of electrospun PU, PU/BB and PU/BB/$CoNO_3$ membranes were randomly distributed without any beads. Image J analysis of the micrographs revealed the fibre diameters of PU, PU/BB and PU/BB/$CoNO_3$ as 1395 ± 133 nm, 563 ± 176 nm and 405 ± 159 nm respectively. The electrospun PU/BB, PU/BB/$CoNO_3$ nanocomposite exhibited a reduced fibre diameter. This is attributed to the added constituents like BB oil and $CoNO_3$. Reduced fibre diameter plays a putative role in enhancing cell adhesion and proliferation. This is majorly due to the diameters of the fabricated fibre which are in the range of the extracellular matrix. A recent study ascribed the reduced diameter (less than 1000 nm) was favourable in case of bone tissue engineering (Chao et al. 2018). Hence, the fabricated composites will be an appropriate candidate for bone tissue growth. Energy dispersive X-ray (EDX) study of electrospun PU/BB/CoNO3 showed cobalt (11.1%) in addition to the oxygen and carbon content.

FTIR analysis

FTIR analysis of PU, PU/BB and PU/BB/$CoNO_3$ was performed to identify the chemical groups and their spectra were shown in Figure 2. The characteristic peaks present in the pristine PU include: broadband at 3,318 cm^{-1} represents NH stretching, peaks at 2,920 cm^{-1} and 2,852 cm^{-1} indicates the CH stretching, twin peaks at 1,730 cm^{-1} and 1,701 cm^{-1} which are attributed to

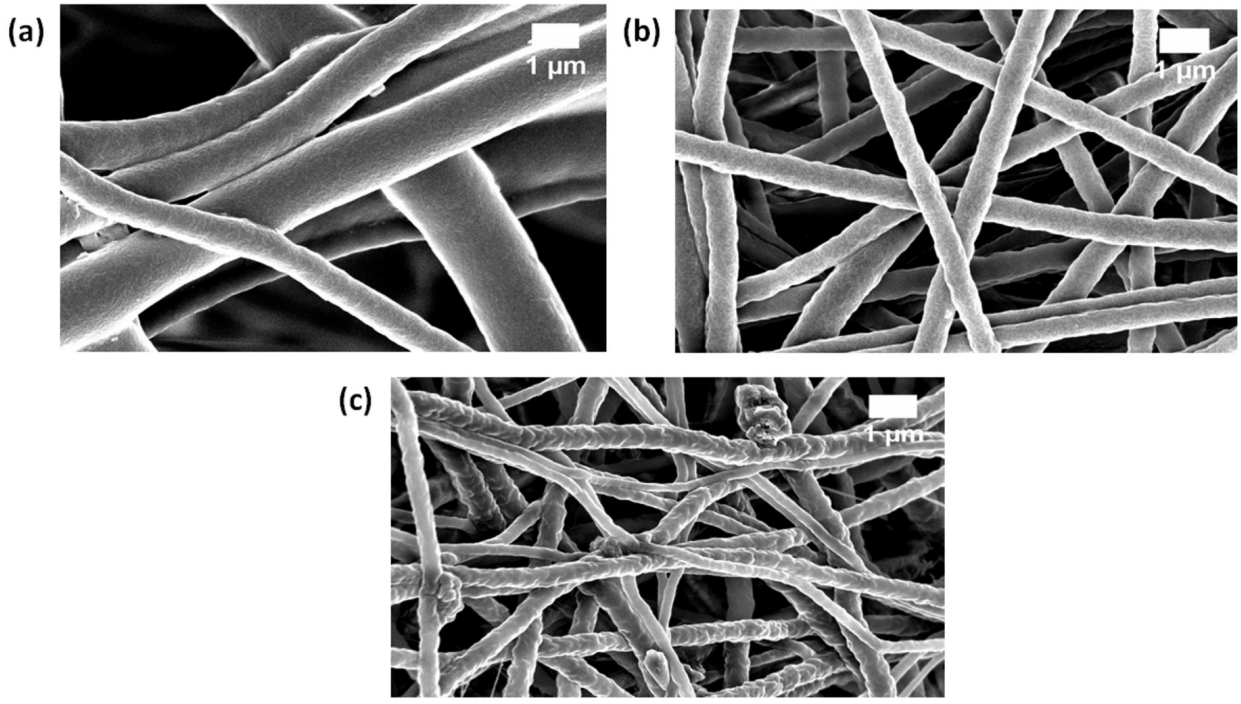

Figure 1. FESEM images of a) PU, b) PU/BB and c) PU/BB/$CONO_3$.

carbonyl stretching, peaks at 1,597 cm–1 and 1,531 cm–1 probably representing the vibrations of NH bending and CN stretching and peaks at 1,221 cm^{-1}, 1,105 cm^{-1} and 770 cm^{-1} that indicates CO stretch (Mani et al. 2018, Chao et al. 2018). Both PE/BB and PE/BB/$CoNO_3$ peaks were similar to that of PU with no new peak's formation. However, the increases in the intensity of peaks were observed with the addition of BB and $CoNO_3$ which was due to the hydrogen bond formation (Unnithan et al. 2012). Further, it's also observed that the change in CH peak shift on adding BB and $CoNO_3$ to the polyurethane matrix (Tijing et al. 2012). The CH peak at 2,920 cm^{-1} in PU was shifted to 2941 cm^{-1} in PU/BB and 2936 cm^{-1} in PU/BB/$CoNO_3$ respectively. Hence, the formation of the hydrogen bond and peak shifts indicates the presence of BB and $CoNO_3$in the polyurethane.

Wettability results

PU scaffold displayed a contact angle of 105° ± 3 and for electrospun PU/BB, PU/BB/CoNO3, it was reported to be 114° ± 1 and 77° ± 2. The results showed that the PU membrane displayed a hydrophobic nature. On adding BB oil, PU scaffold turned hydrophobic whereas adding $CONO_3$ to the PU/BB, wettability was reversed. The addition of $CoNO_3$ into the PU/BB scaffold favours the hydrophilic nature of the composite scaffold. A hydrophilic scaffold favours enhanced cell growth and differentiation whereas it is limited in the hydrophobic scaffold as it retards the movement of cell culture medium. Further, while seeding the cells, a homogeneous distribution is obtained in a hydrophilic scaffold favouring the formation of well-engineered tissues (Yassin et al. 2016). In addition to this, the observed wettability is in the optimal range suitable for osteoblast adhesion (Wei et al. 2009). Hassan et al. (2014) developed a scaffold using poly (ε-caprolactone, PCL) and hydroxyapatite (HA) nanofibres. Hydrophilic nature of the PCL/HA was found to be encouraging in bone tissue engineering. PE/BB/$CoNO_3$ with improved wettability seems to be a viable option for bone tissue engineering.

Thermal analysis

The thermal analysis of the electrospun PU, PU/BB, PU/BB/$CoNO_3$ scaffolds were shown in Figure 3. Electrospun polyurethane displayed three stages of degradation with the first onset from 290°C to 375°C, second from 375°C to 414°C and the third one from 414°C to 650°C. In the case of the PU/BB, there were two stages of degradation first one from 296°C to 365°C and the second one from 365°C to 409°C. PU/BB/$CoNO_3$ depicted four stages of degradation. The four stages of degradation were as follows: 195°C to 250°C, 250°C to 350°C, 350°C to 510°C and 510°C to 615°C. The thermal stability of the PU membrane was increased with the addition of BB and then decreased while adding $CoNO_3$. The decrease in the degradation temperature was because of vaporization of volatile molecules (H_2O) present in the cobalt nitrate. Further, the DTG curves of the electrospun membrane and their curves were shown in Figure 4. Peaks of DTG indicated the mass loss from the samples. The height of the peaks indicated the rate at which degradation takes place. In our case, polyurethane expressed a degradation rate of 0.18 mg/min followed by PU/BB (0.2 mg/min) and PU/BB/ $CoNO_3$ (0.11 mg/min). This clearly evidences that the slower degradation properties of the developed composite (PU/BB/ $CoNO_3$). It could be inferred, based on the change in peak intensity between the polyurethane and the composite samples, BB and $CoNO_3$are integrated into the polyurethane backbone.

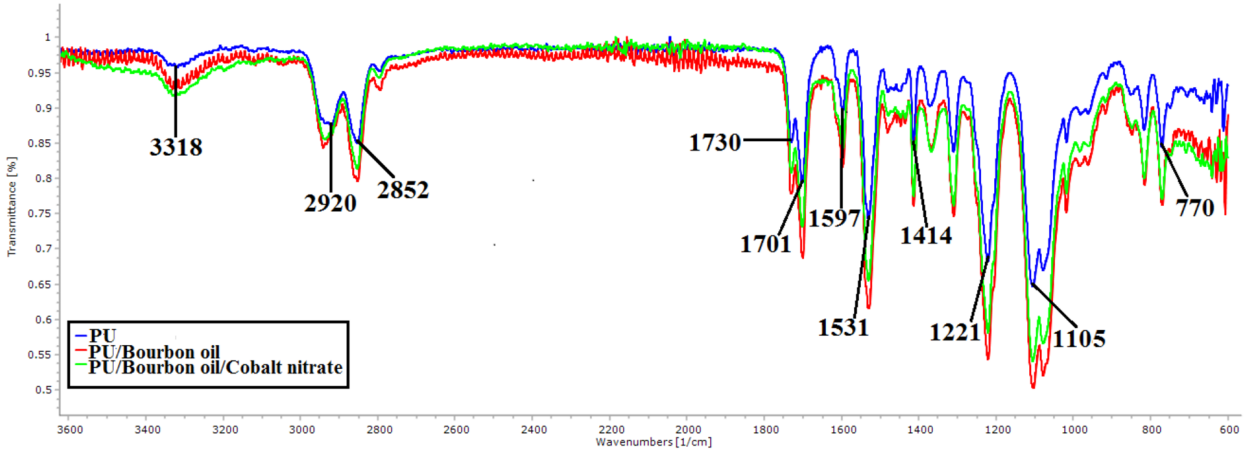

Figure 2. FTIR images of PU, PU/BB and PU/BB/$CONO_3$.

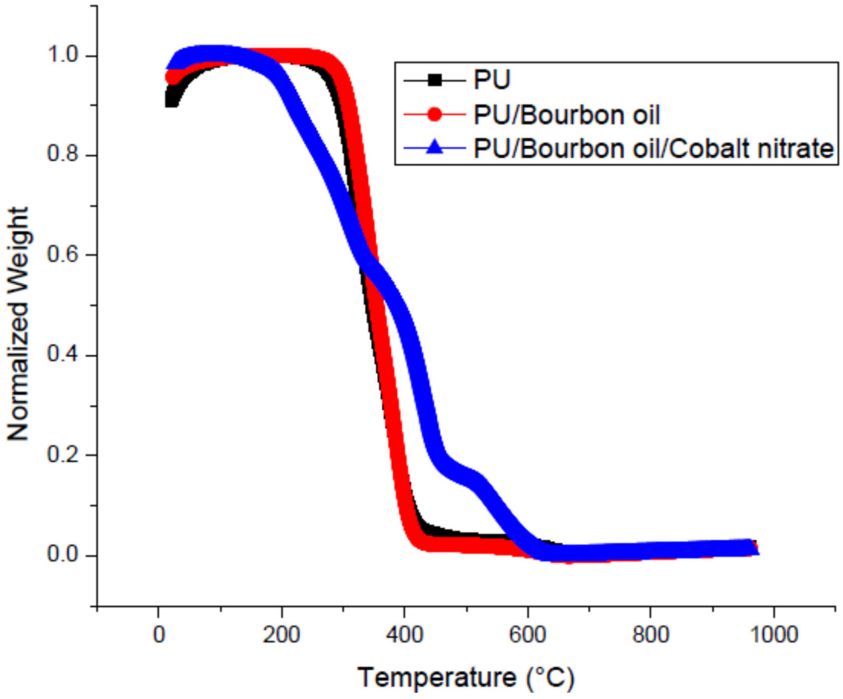

Figure 3. TGA curve of a) PU, PU/BB and PU/BB/$CONO_3$.

Surface analysis

The 3D surface images of developed PU, PU/BB, PU/BB/$CoNO_3$ scaffold are presented in Figure 5. The average roughness (Ra) of the PU membrane was observed to be 854 ± 32 nm. PU/BB and PU/BB/$CoNO_3$ scaffolds displayed Ra of 565 ± 37 nm and 538 ± 155 nm respectively. PU/BB and PU/BB/$CoNO_3$ were smoother than the pristine PU. Kim et al. (2016) found that scaffolds rendering smaller fibre diameter would possess smoother surfaces compared to the larger fibre diameter ones. The smaller fibre diameter due to the addition of BB and $CoNO_3$ might have favoured the decrease in the surface roughness. Ribeiro et al. (2015) showed that smooth surface enhances the osteoblast proliferation than rough surfaces insinuating the potential of newly developed scaffolds in bone repair.

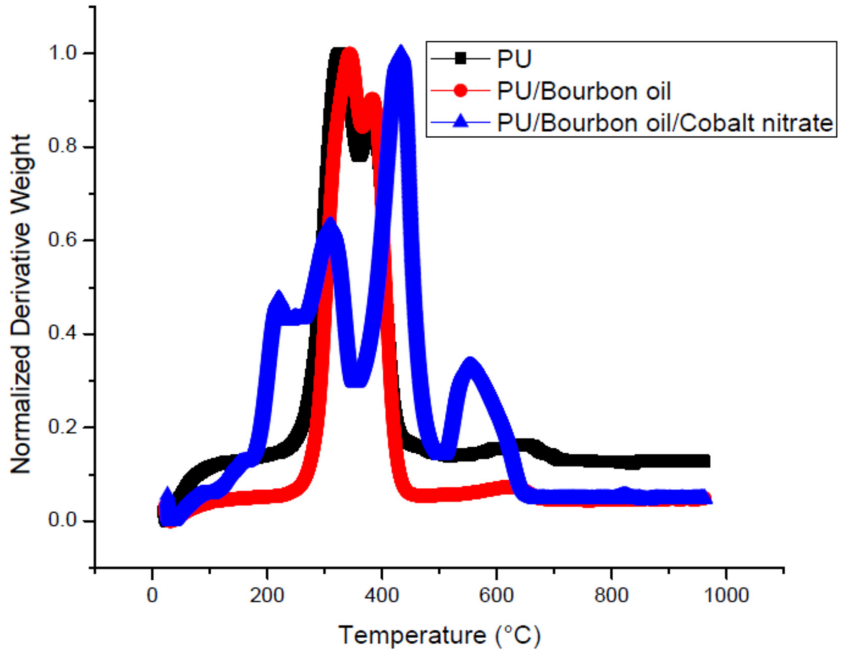

Figure 4. DTG curve of PU, PU/BB and PU/BB/$CONO_3$.

Tensile analysis

The pristine PU nanofibres exhibited a tensile strength of 6.16 MPa whereas PU/BB and PU/BB/$CoNO_3$ displayed a strength of 8.92 MPa and 12.97 MPa respectively (Figure 6). Addition of BB and $CoNO_3$ enhanced the strength of the PU. Literature cites that the smaller fibre diameter would favour the mechanical strength (Mani et al. 2019, Sheikh et al. 2010) and this is in line with our observations from FESEM where we had reported smaller diameter for the composites rather than the PU. Shanmugavel et al. (2014) reported that their prepared scaffold with the strength of about 4MPa suitable for bone tissue engineering. Our composite membranes displayed enhanced strength than the reported scaffold strength indicating its dominance for bone tissue engineering.

Coagulation results

The APTT and PT time for electrospun PU, PU/BB, PU/BB/$CoNO_3$ scaffold were shown in Figure 7a and 7b. The coagulation times were determined through APTT assay and for PU scaffold it was 176 ± 2 s while PU/BB, PU/BB/$CoNO_3$ scaffold, it was found to be 204 ± 3 s and 201 ± 1 s respectively. Similarly, the blood clotting time determined through PT assay for PU scaffold was 94 ± 2 s and for electrospun PU/BB, PU/BB/$CoNO_3$ scaffold, it was found to be 107 ± 2 s and 104 ± 3 s respectively. For the PU, the haemolytic percentage was calculated to be 2.83% and for PU/BB, PU/BB/$CoNO_3$ scaffolds, it was found to be 1.55% and 1.66%, respectively as presented in Figure 7c. The delay in blood clotting time was owing to the presence of BB and $CoNO_3$ into the PU. Initially, when BB is added to the PU matrix, the surface turned to be more hydrophobic which enabled the irreversible adhesion of plasma proteins resulting in a delay of blood coagulation times. However, when $CoNO_3$ is added, the surface turned to be hydrophilic resulting in slight reduction, however, it was still higher than that of the PU. This is because of change in the polar and apolar regions of the PU/BB/$CoNO_3$ scaffold (Szycher 1991). Studies had suggested that the scaffold with smaller fibre diameter and hydrophobicity might influence the anticoagulant behaviour (Li et al. 2019). Our fabricated composites with smaller

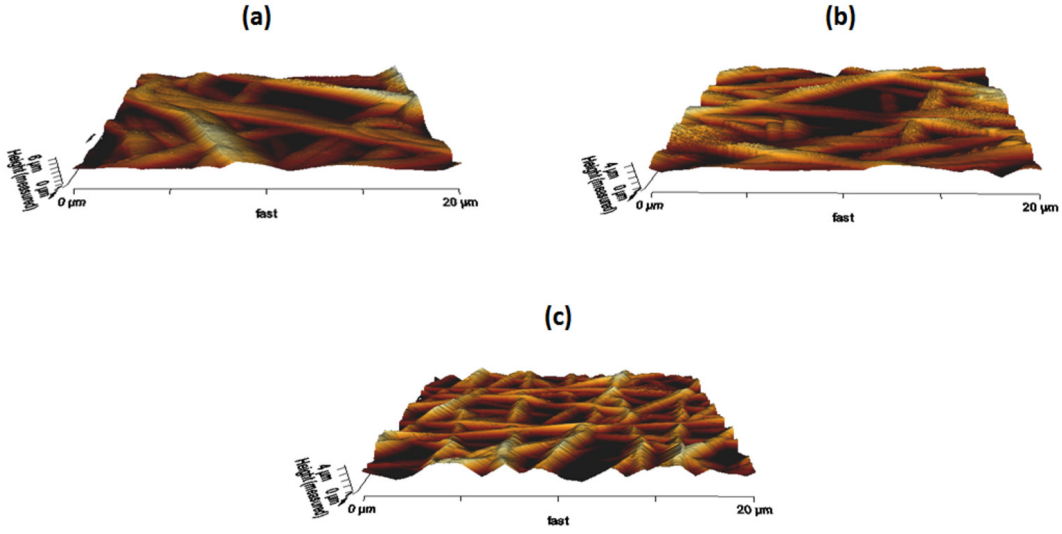

Figure 5. AFM images of a) PU, b) PU/BB and c) PU/BB/$CONO_3$.

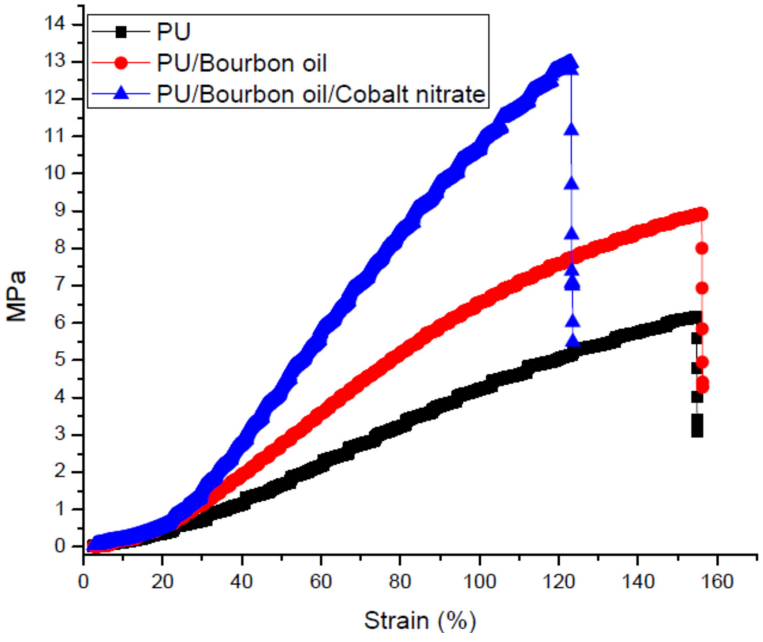

Figure 6. Tensile curves of PU, PU/BB and PU/BB/$CONO_3$.

fibre diameter (PU/BB and PU/BB/$CONO_3$) and hydrophobic nature (PU/BB) might have an influence in the enhanced anticoagulant nature.

Bone mineralisation testing

Calcium depositions of the fabricated PU, PU/BB, PU/BB/$CoNO_3$ were determined through FESEM imaging and EDX spectra as shown in Figure 8. The fabricated composites showed enhanced progress of mineralization than the pristine PU. The amount of calcium deposition for the pristine PU was found to be 2.4% and for electrospun PU/BB, PU/BB/$CoNO_3$ showed a calcium weight percentage of 8.6% and 11% respectively. Hence, the presence of BB and $CoNO_3$ accelerated the calcium deposition of the PU signifying PU/BB, PU/BB/$CoNO_3$ as probable alternatives in bone reconstruction. Hassan et al. (2014) electrospun a PCL scaffold added with hydroxyapatite for bone tissue engineering. It was found that the hydroxyapatite addition enhanced the calcium deposition than the pure PCL which resembles our findings. Hence, the enhanced calcium deposition of the electrospun

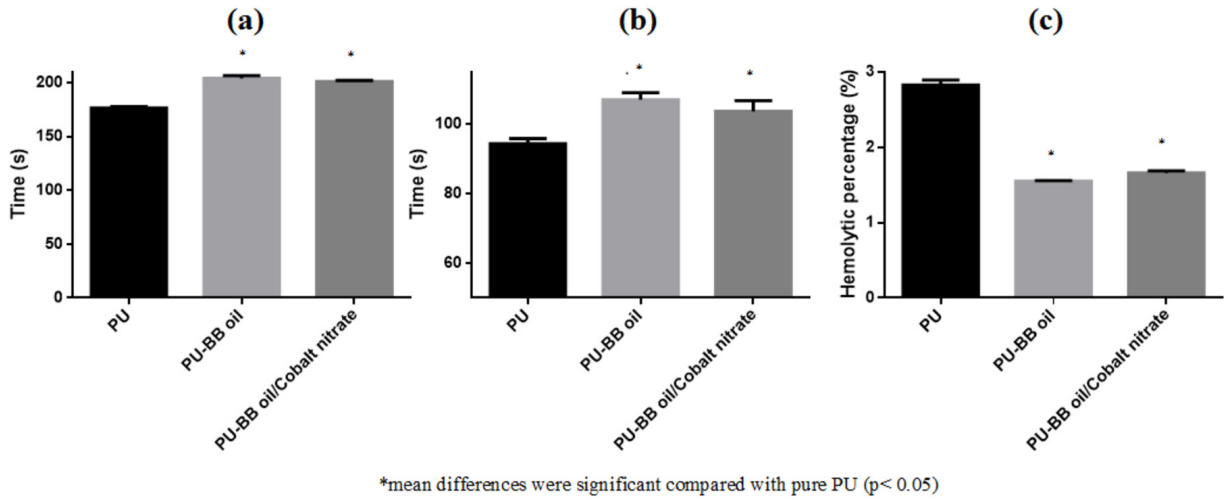

Figure 7. a) APTT, b) PT and c) Hemolytic index of PU, PU/BB and PU/BB/$CONO_3$.

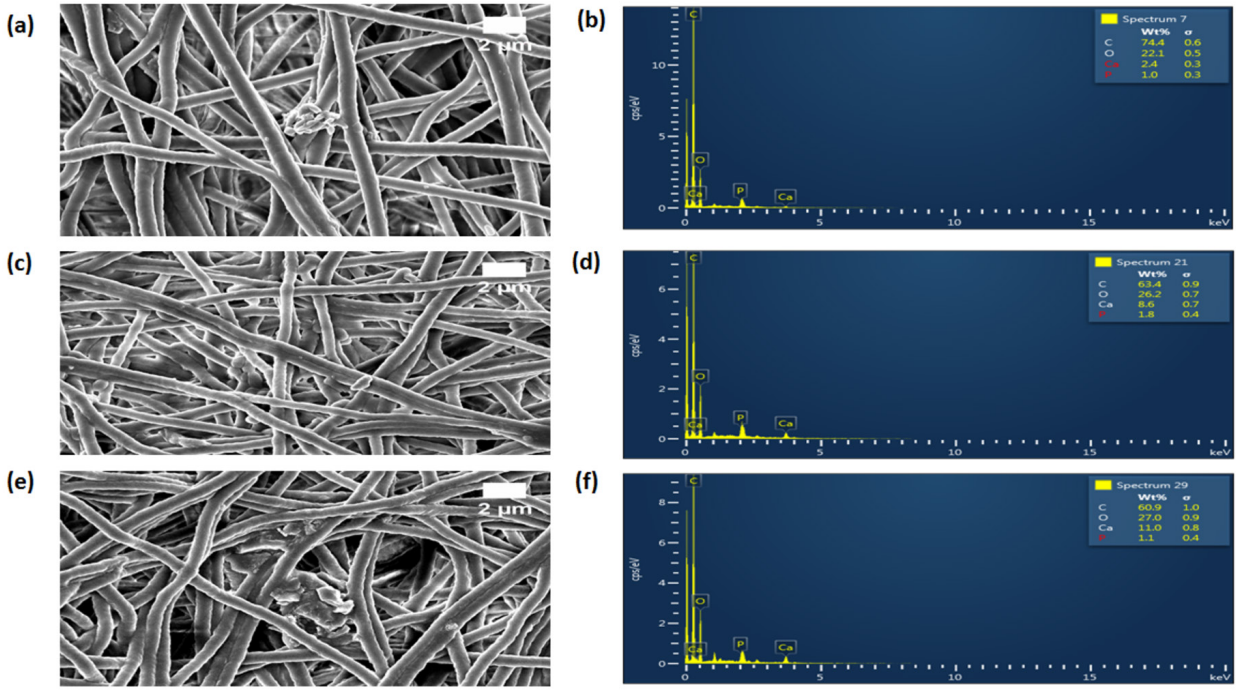

Figure 8. Bone mineralization testing a,c,e) FESEM images of electrospun membranes and b,d,f) EDX spectrum of electrospun membranes.

composites might be exploited for bone tissue engineering scaffolds.

CONCLUSIONS

Electrospun scaffolds of the PU, PU/BB and PU/BB/$CoNO_3$ were successfully fabricated by optimizing the solution and process parameters. The fabricated PU/BB, PU/BB/$CoNO_3$ scaffolds displayed relevant physicochemical properties like fibre diameter, wettability and roughness which can be tailored for bone tissue engineering. Further, PU/BB, PU/BB/ $CoNO_3$ scaffolds have better blood compatibility and also enhanced bone formation ability. However, it requires

further experimentation of how the developed scaffold reacts with the osteoblast cells which may further throw lights on the compatibility of scaffolds with the bone cells.

Acknowledgments

Authors have not received any funding for this specific work. The authors have declared no conflict of interest.

REFERENCES

AMINI AR, LAURENCIN CT & NUKAVARAPU SP. 2012. Bone tissue engineering, recent advances and challenges. Crit Rev Biomed Eng 40(5).

BOKOV AE, MLYAVYKH SG, SHIROKOVA NY, DAVYDENKO DV & ORLINSKAYA NY. 2018. Current Trends in the Development of Materials for Bone Grafting and Spinal Fusion. Современныетехнологии в медицине, 10(4 (eng)).

CHANG EL, SIMMERS C & KNIGHT DA. 2010. Cobalt complexes as antiviral and antibacterial agents. Pharm 3(6): 1711-1728.

CHAO CY, MANI MP & JAGANATHAN SK. 2018. Engineering electrospun multicomponent polyurethane scaffolding platform comprising grapeseed oil and honey/propolis for bone tissue regeneration. PLoS One 13(10).

GONG T, XIE J, LIAO J, ZHANG T, LIN S & LIN Y. 2015. Nanomaterials and bone regeneration. Bone Res 3: 15029.

HAIDER A ET AL. 2020. Advances in the scaffolds fabrication techniques using biocompatible polymers and their biomedical application, A technical and statistical review. J Saudi Chem Soc 24(2): 186-215.

HASSAN MI, SULTANA N & HAMDAN S. 2014. Bioactivity assessment of poly (ε-caprolactone)/hydroxyapatite electrospunfibres for bone tissue engineering application. J Nanomater 2014.

HONG J, YEO M, YANG GH & KIM G. 2019. Cell-Electrospinning and Its Application for Tissue Engineering. Int J Mol Sci 20(24): 6208.

HO-SHUI-LING A, BOLANDER J, RUSTOM LE, JOHNSON AW, LUYTEN FP & PICART C. 2018. Bone regeneration strategies, Engineered scaffolds, bioactive molecules and stem cells current stage and future perspectives. Biomater 180: 143-162.

JAGANATHAN SK, MANI MP & KHUDZARI AZ. 2019. Electrospun combination of peppermint oil and copper sulphate with conducive physico-chemical properties for wound dressing applications. Polym 11(4): 586.

JAGANATHAN SK, MANI MP, ISMAIL AF & AYYAR M. 2017. Manufacturing and characterization of novel electrospun composite comprising polyurethane and mustard oil scaffold with enhanced blood compatibility. Polym 9(5): 163.

JAGANATHAN SK, MANI MP, PALANIAPPAN SK & RATHANASAMY R. 2018. Fabrication and characterisation of nanofibrous polyurethane scaffold incorporated with corn and neem oil using single stage electrospinning technique for bone tissue engineering applications. J Polym Res 25(7): 146.

JUN I, HAN HS, EDWARDS JR & JEON H.2018. Electrospun fibrous scaffolds for tissue engineering, Viewpoints on architecture and fabrication. Int J Mol Sci 19(3): 745.

KIM HH, KIM MJ, RYU SJ, KI CS & PARK YH. 2016. Effect of fibre diameter on surface morphology, mechanical property, and cell behavior of electrospun poly (ε-caprolactone) mat. Fibre Polym 17: 1033-1042.

KUNDU J, PATI F, SHIM JH & CHO DW. 2014. Rapid prototyping technology for bone regeneration. Rapid Prototyp Biomater: 289-314.

LI G, LI P, CHEN Q, MANI MP & JAGANATHAN SK. 2019. Enhanced mechanical, thermal and biocompatible nature of dual component electrospun nanocomposite for bone tissue engineering. PeerJ 7: e6986.

LIU H, DING X, ZHOU G, LI P, WEI X & FAN Y. 2013. Electrospinning of nanofibres for tissue engineering applications. J Nanomater 2013: Article ID 495708. https://doi.org/10.1155/2013/495708.

MADANI M & HAMOUDA AS. 2016. Using Electrospinning Technique for Preparation of Cobalt Hydroxide Nanoparticles. Qatar Found Annual Res Conf Proceed 1, EEPP1129.

MANI MP, JAGANATHAN SK, KHUDZARI AZ & PRABHAKARAN P. 2019. Development of advanced nanostructured polyurethane composites comprising hybrid fillers with enhanced properties for regenerative medicine. Polym Test 73: 12-20.

MANI MP, JAGANATHAN SK, KHUDZARI AZ, RATHANASAMY R & PRABHAKARAN P. 2018. Single-stage electrospun innovative combination of polyurethane and neem oil, synthesis, characterization and appraisal of blood compatibility. J Bioact Comp Polym 33(6): 573-584.

NEFFE AT, JULICH-GRUNER KK & LENDLEIN A. 2014. Combinations of biopolymers and synthetic polymers for bone regeneration. Biomater Bone Regen: 87-110.

PARK KH, KIM S, HWANG MJ, SONG HJ & PARK YJ. 2017. Biomimetic fabrication of calcium phosphate/chitosan nanohybrid composite in modified simulated body fluids. Express Polymer Lett 11(1): 14-20.

PERRONE MS. 2012. Electrospun Proton-Conducting Nanofibre Mats for use in Advanced Direct Methanol Fuel Cell Electrodes. Thesis submitted to Worcester Polytechnic Institute. (Unpublished).

RIBEIRO C, SENCADAS V, AREIAS AC, GAMA FM & LANCEROS-MENDEZ S. 2015. Surface roughness dependent osteoblast and fibroblast response on poly (l-lactide) films and electrospun membranes. J Biomed Mater Res Part A 103(7): 2260-2268.

SHANMUGAVEL S, REDDY VJ, RAMAKRISHNA S, LAKSHMI BS & DEV VG. 2014. Precipitation of hydroxyapatite on electrospunpolycaprolactone/aloe vera/silk fibroin nanofibrous scaffolds for bone tissue engineering. J Biomater Appl 29(1): 46-58.

SHEIKH FA, BARAKAT NA, KANJWAL MA, JEON SH, KANG HS & KIM HY. 2010. Self synthesize of silver nanoparticles in/on polyurethane nanofibres, Nano-biotechnological approach. J Appl Polym Sci 115(6): 3189-3198.

SZYCHER M. 1991. High performance biomaterials, a complete guide to medical and pharmceutical applications. Boca Raton, CRC Press.

TIJING LD, RUELO MTG, AMARJARGAL A, PANT HR, PARK CH, KIM DW & KIM CS. 2012. Antibacterial and superhydrophilic electrospun polyurethane nanocomposite fibres containing tourmaline nanoparticles. Chem Eng J 197: 41-48.

UNNITHAN AR, PICHIAH PT, GNANASEKARAN G, SEENIVASAN K, BARAKAT NA, CHA YS, JUNG CH, SHANMUGAM A & KIM HY. 2012. Emu oil-based electrospun nanofibrous scaffolds for wound skin tissue engineering. Colloids Surf A, Physicochem Eng Asp 415: 454-460.

VASITA R & KATTI DS. 2006. Nanofibres and their applications in tissue engineering. International J Nanomed 1(1): 15.

VERMA RS, RAHMAN LU, VERMA RK, CHAUHAN A & SINGH A. 2013. Essential oil composition of Pelargonium graveolensL'Her ex Ait. cultivars harvested in different seasons. J Essen Oil Res 25(5): 372-379.

WEI J, IGARASHI T, OKUMORI N, IGARASHI T, MAETANI T, LIU B & YOSHINARI M. 2009.Influence of surface wettability on competitive protein adsorption and initial attachment of osteoblasts. Biomed Mater 4(4): 045002.

WU C, ZHOU Y, FAN W, HAN P, CHANG J, YUEN J, ZHANG M & XIAO Y. 2012. Hypoxia-mimicking mesoporous bioactive glass scaffolds with controllable cobalt ion release for bone tissue engineering. Biomater 33(7): 2076-2085.

YASSIN MA, LEKNES KN, SUN Y, LIE SA, FINNEWISTRAND A & MUSTAFA K. 2016. Surfactant tuning of hydrophilicity of porous degradable copolymer scaffolds promotes cellular proliferation and enhances bone formation. J Biomed Mater Res A 104(8): 2049-2059.

How to cite

JAGANATHAN SK & MANI MP. 2021. Investigation of attributes of bourbon oil and cobalt nitrate constituted electrospun nanoscaffolds for blood compatibility and in vitro bone formation. An Acad Bras Cienc 93: e20201140. DOI 10.1590/0001-3765202120201140.

Manuscript received on July 25, 2020;
accepted for publication on December 16, 2020

SARAVANA K. JAGANATHAN[1,2]
https://orcid.org/0000-0002-2785-137X

MOHAN P. MANI[3]
https://orcid.org/0000-0002-6048-4241

[1]University of Hull, Department of Engineering, Faculty of Science and Engineering, HU6 7RX, Hull, U.K.

[2]Universiti Teknologi Malaysia, School of Electrical Engineering, Faculty of Engineering, 81310, Johor Bahru, Malaysia

[3]Universiti Teknologi Malaysia, School of Biomedical Engineering and Health Sciences, Faculty of Engineering, 81310, Skudai, Malaysia

Correspondence to: **Saravana Kumar Jaganathan**
E-mail: s.k.jaganathan@hull.ac.uk

Author contributions

Conceptualization: S.K.J; Data curation: M.P.M and S.K.J; Formal analysis: M.P.M and S.K.J; Investigation: M.P.M; Methodology: M.P.M and S.K.J; Project administration: S.K.J; Resources and software: S.K.J; Supervision: S.K.J; Validation: M.P.M and S.K.J; Visualization: S.K.J; Writing—original draft: M.P.M.; Writing—review & editing: M.P.M and S.K.J.